Eur. Phys. J. D **14**, 167–172 (2001)

THE EUROPEAN PHYSICAL JOURNAL D

EDP Sciences

Selective preparation of ground state wave-packets: a theoretical analysis of femtosecond pump-dump-probe experiments on the potassium dimer

Z.W. Shen, T. Chen, M. Heid, W. Kiefer, and V. Engel[a]

Institut für Physikalische Chemie, Universität Würzburg, Am Hubland, 97074 Würzburg, Germany

Received 27 September 2000 and Received in final form 21 November 2000

Abstract. We present simulations on pump-dump-probe experiments performed on the potassium dimer. The interaction of two time-delayed laser pulses prepares vibrational wave packets in the electronic ground state. The quantum calculations reveal to what extent it is possible to prepare a ground state superposition of states with high *versus* low vibrational quantum numbers by changing the pump-dump delay time. It is shown that transient signals may exhibit interference effects which are due to characteristics of ground state wave-packets composed of two components showing different vibrational dynamics. In this way the signals are able to yield information about vibrational overtone motion.

PACS. 31.70.Hq Time-dependent phenomena: excitation and relaxation processes, and reaction rates – 33.80.Wz Other multiphoton processes

1 Introduction

The laser control of chemical reactions is subject of intense research work and discussion [1,2]. Two control schemes have been extensively used in theoretical and experimental studies. One is the *Brumer-Shapiro* scheme [3,4] which employs two lasers with well defined frequencies and relative phases. In this way electronic transitions in molecules can be induced where a common final state is reached *via* two excitation pathways. By controlling the relative phase between the two radiation sources one is able to induce interferences, thereby enhancing or suppressing the population of certain final states. This scenario can be compared to a two-slit experiment where, in the control scheme, the distance of the slits corresponds to the relative phase of the two laser beams.

A time-dependent aspect appears in a more direct way in the *Tannor-Rice-Kosloff* control scheme [5,6]. Here, a first laser pulse prepares a non-stationary state in a molecule. Since this wave-packet changes its location on the potential-energy curve of the state which was excited, a second, time-delayed pulse is able to induce effective transitions to another electronic state at certain delay times. This scheme is, in fact, not basically different from the Brumer-Shapiro approach. In the former case we might think of a multiple slit experiment since there are many pathways leading from a single initial state *via* a manifold of intermediate states to a final state. The various phases are determined by the time-evolution in the intermediate state.

[a] e-mail: voen@phys-chemie.uni-wuerzburg.de

Recently, an exciting control experiment was performed in the Gerber laboratory [7] which, employing feedback and evolutionary algorithms [8], showed that the idea of coherent control indeed works in larger molecular systems. As one experimental result it was shown, that the branching ratio of chemically different species can be controlled to a large extent.

In the present study we treat the simple, but by no means trivial, case of a diatomic molecule. The objective is to investigate the preparation and detection of vibrational ground state wave packets. In doing so we analyze experiments on the K_2 molecule which were performed recently in our laboratory [9–11]. The potassium dimer has been investigated using femtosecond time-resolved spectroscopy by several groups [12–15]; for the application of a learning algorithm to the same molecule see the recent paper by Hornung *et al.* [16]. The experimental set-up used in our time resolved experiments was described before and we will not repeat the details here. Let us, instead, discuss the principle of the excitation and detection mechanism regarding the scheme presented in Figure 1. A femtosecond pump pulse couples the electronic ground state $|g\rangle$ and an excited state $|e\rangle$ of the molecule. Due to a high field strength (intensities up to 10 GW/cm^2 were used in the experiment) this results in the preparation of an excited state-($|\psi_e\rangle$) and a ground state-wave packet ($|\psi_g\rangle$). Similar intensity effects have been found before in the Na_2 [17] and also the K_2 [18] molecule.

At a variable delay time τ_1, a second short laser pulse (dump pulse) is sent through the sample. The carrier frequency is chosen such that it prepares a packet in the

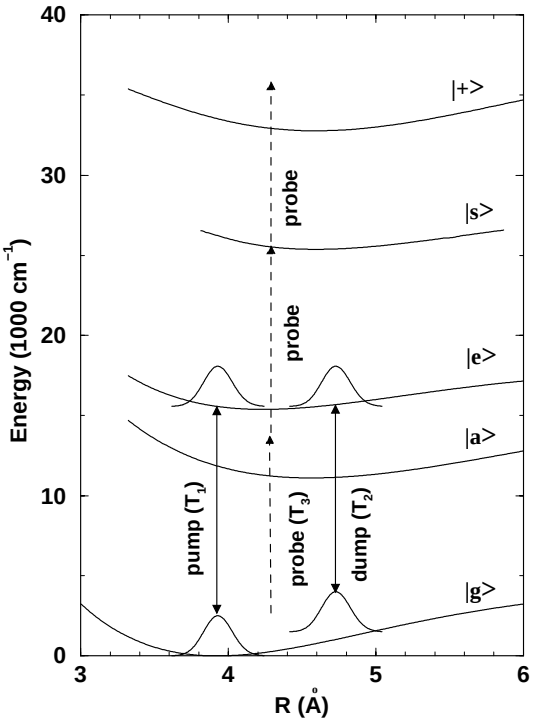

Fig. 1. Excitation scheme of a three pulse experiment on the K_2 molecule. The pump- and dump-pulses, which are centered around times T_1, T_2 couple the electronic ground state $|g\rangle$ and an excited state $|e\rangle$. The probe pulse, centered at time T_3, induced a three photon ionization process.

electronic ground state consisting of a coherent superposition of states with high vibrational quantum numbers. Finally, a third laser pulse (probe) induces ionization from the electronic ground state *via* a three-photon absorption process. The possible excitation of other electronically excited states in the pump-dump process will not be discussed here, for details see references [9–11].

The experimental ionization signals exhibit traces of wave-packet motion in the electronic ground state. In particular, vibrational frequencies corresponding to quantum numbers of $v'' = 0,\ 1$ and $v'' = 11-15$ were found from a Fourier analysis of the signals. The ratio of these contributions could be controlled by changing the pump-dump delay.

In this paper we want to analyze the experimental results thereby arriving at a deeper insight into the pump-dump process and the control of the various ground state wave-packets. The paper is organized as follows: in Section 2 we describe the theoretical treatment of the system and the model. The numerical results are presented in Section 3 and 4 gives a summary.

2 Theory and model

We describe the interaction of three laser pulses with K_2 molecules, as illustrated in Figure 1. A first ultrashort pulse (pump) couples the electronic ground state $|g\rangle$ ($^1\Sigma_g^+$) with the excited state $|e\rangle$ ($^1\Pi_u$). A second, time-delayed pulse (dump) of different wavelength introduces another coupling between these two electronic states. Finally, the third pulse (probe) with yet another center wavelength induces a three-photon ionization process. The latter proceeds (one-photon) non-resonant *via* the electronic state $|a\rangle$ ($^1\Sigma_u^+$) but (two-photon) resonant with the state $|s\rangle$ ($5^1\Sigma_g^+$). We note that there is another state ($6^1\Sigma_g^+$) which is energetically close to $|s\rangle$. Our calculations showed that ionization signals involving this state are very similar to the ones obtained with the $|s\rangle$ ($5^1\Sigma_g^+$) state so that we feel no need to regard this second ionization pathway in what follows. This neglection ignores interference effects which arise from the coherent superposition of ionization amplitudes resulting from the two ionization pathways (*via* the $5^1\Sigma_g^+$ and $6^1\Sigma_g^+$ state). However, since the experiments involve an average over many laser shots and are not performed with phase-locked pulses, these interferences are not detected. There are other femtosecond time-resolved experiments which employ such interferences to characterize the nuclear dynamics, see *e.g.* [19–23].

Let us first concentrate on the population transfer which is induced by the pump- and dump-pulses. In what follows, only the vibrational degree-of-freedom is considered. The Hamiltonian involving two electronic states reads

$$H = |e\rangle\, H_e\, \langle e| + |g\rangle\, H_g\, \langle g| + |e\rangle\, W_{eg}(t)\, \langle g| + |g\rangle\, W_{ge}(t)\, \langle e|. \quad (1)$$

Here $H_{e,g}$ are the Hamiltonians for the nuclear motion in $|e\rangle, |g\rangle$, respectively. They contain the potentials $V_{e,g}$, as displayed in Figure 1. The light-matter interaction is obtained within the dipole-approximation as (atomic units are used throughout)

$$W_{eg}(t) = -\mu_{eg}\, \{E_1 f(t-T_1)\cos(\omega_1(t-T_1)) + E_2 f(t-T_2)\cos(\omega_2(t-T_2))\}\cdot \quad (2)$$

The projection of the transition dipole-moment on the laser polarization vector is denoted as μ_{eg}. In our calculation we employ the rotating-wave-approximation. Using, furthermore, the Condon-approximation, we set all dipole moments to a constant value of one. The pump ($i = 1$) and dump ($i = 2$) fields are characterized by envelope functions $f(t)$ centered at times T_i, a carrier frequency ω_i and a field strength E_i. The latter is set to a value corresponding to a peak intensity of $I = 2 \times 10^{10}$ W/cm^2.

We solve the coupled equations for the vibrational motion in the two electronic states numerically using the split-operator method [24]. Since we regard molecular beam experiments where the dimers are produced vibrationally cold, the initial state of the system is taken as the vibrational ground state with quantum number $v'' = 0$. The same Gaussian envelope function $f(t)$ is employed for the pump- and dump-pulse. The width of the temporal shape function is chosen such that the full-width-at-half-maximum (FWHM) of the corresponding intensity autocorrelation function is 70 fs.

To simulate the pump-probe transients we calculate signals under the following assumptions:

(a) the population in state $|s\rangle$ is proportional to the ion signal;
(b) the two-photon non-resonant transition $|s\rangle \leftarrow |g\rangle$ can be treated as an effective one-photon transition.

The approximation (a) is reasonable since the state $|s\rangle$ is directly coupled to the ionization continuum *via* the molecule-field interaction. Assumption (b) can be justified as follows: using second-order perturbation theory, the state in $|s\rangle$ is obtained as

$$|\psi_{\rm s}(t)\rangle = -\int_{-\infty}^{t} {\rm d}t'\; U_{\rm s}(t-t')\; W_{\rm sa}(t') \times \int_{-\infty}^{t'} {\rm d}t''\; U_{\rm a}(t'-t'')\; W_{\rm ag}(t'')\; U_{\rm g}(t'')|\psi_{\rm g}\rangle. \quad (3)$$

Here U_n denotes the propagator in the electronic state $|n\rangle$ and the molecule-field interaction has the form

$$W_{nm}(t) = -\frac{\mu_{nm}}{2} E_3 f(t-T_3) {\rm e}^{-{\rm i}\omega_3(t-T_3)}, \quad (4)$$

where the index 3 characterizes the probe pulse and we included only the term responsible for absorption. The initial state $|\psi_{\rm g}\rangle$ represents the vibrational ground state in $|g\rangle$.

We now evaluate equation (3) using a square pulse for $f(t)$ starting at the delay-time $t = \tau_2$ which, for convenience, will be set to zero, and ending at $t = T$. In doing so, we adopt the approximation to neglect all kinetic energy operators which appear in the propagators [25–29]. This yields

$$|\psi_{\rm s}(T)\rangle = -E_3^2\, \frac{{\rm e}^{-{\rm i}V_{\rm s}T}}{4{\rm i}(V_{\rm a}-V_{\rm g}-\omega_3)} \left\{ \frac{{\rm e}^{{\rm i}(V_{\rm s}-V_{\rm g}-2\omega_3)T}-1}{{\rm i}(V_{\rm s}-V_{\rm g}-2\omega_3)} - \frac{{\rm e}^{{\rm i}(V_{\rm s}-V_{\rm a}-\omega_3)T}-1}{{\rm i}(V_{\rm s}-V_{\rm a}-\omega_3)} \right\} |\mu_{\rm sa}\mu_{\rm ag}\psi_{\rm g}(0)\rangle \cdot \quad (5)$$

Since in our case we have $V_{\rm s} - V_{\rm g} - 2\omega_3 \sim 0$, the first term in equation (5) has the form of a resonant contribution to the excited state $|\psi_{\rm s}(T)\rangle$. Neglection of the second (non-resonant) term yields

$$|\psi_{\rm s}(T)\rangle = \frac{E_3^2}{4}\, {\rm e}^{-{\rm i}V_{\rm s}T}\, \frac{1}{2(V_{\rm a}-V_{\rm g}-\omega_3)} \times \frac{{\rm e}^{{\rm i}(V_{\rm s}-V_{\rm g}-2\omega_3)T}-1}{V_{\rm s}-V_{\rm g}-2\omega_3}\, |\mu_{\rm sa}\mu_{\rm ag}\psi_{\rm g}(0)\rangle \cdot \quad (6)$$

Let us next regard a resonant one-photon transition $|2\rangle \leftarrow |1\rangle$ induced by a field of the form $E(t) = (E/2)f(t){\rm e}^{-{\rm i}\omega t}$. The first-order state

$$|\psi_2(t)\rangle = \frac{-1}{2{\rm i}} \int_0^t {\rm d}t'\; U_2(t-t')\mu_{21}E(t')U_1(t')|\psi_{\rm g}(0)\rangle \quad (7)$$

may be evaluated for a square pulse within the same assumptions as above to obtain

$$|\psi_2(T)\rangle = E\frac{E}{2}\, {\rm e}^{-{\rm i}V_2T} \frac{{\rm e}^{{\rm i}(V_2-V_1-\omega)T}-1}{V_2-V_1-\omega}\, |\mu_{21}\psi_{\rm g}(0)\rangle \cdot \quad (8)$$

This expression is similar to equation (6) if the obvious substitutions are made. A difference lies in the appearance of the function $(V_{\rm a} - V_{\rm g} - \omega_3)^{-1}$ which is responsible for the weak amplitude for a non-resonant multi-photon transition. It turned out that in our case the coordinate dependence of this function can be ignored so that, in what follows, we set it to a constant. Within this approximation we may now return to arbitrary pulse shapes to arrive at an approximate expression for the wave function in $|s\rangle$ as

$$|\psi_{\rm s}(t)\rangle \sim F_{\rm sg}\, |\mu_{\rm sa}\mu_{\rm ag}\psi_{\rm g}(0)\rangle, \quad (9)$$

where F is defined as

$$F_{\rm sg}(R) = \frac{E_3^2}{4} \int_{-\infty}^{+\infty} {\rm d}t\; f(t){\rm e}^{{\rm i}(V_{\rm s}(R)-V_{\rm g}(R)-2\omega_3)t}, \quad (10)$$

where we have ignored phase factors of modulus one. The transient signal $S(\tau_2)$ is now evaluated in the coordinate representation as the population in state $|s\rangle$ prepared by the time-delayed probe pulse:

$$S(\tau_2) = \int {\rm d}R\; |F_{\rm sg}(R)\mu_{\rm sa}\mu_{\rm ag}\psi_{\rm g}(R,\tau_2)|^2. \quad (11)$$

The interpretation of the latter equation is as follows: the signal $S(\tau_2)$ measures the probability density $|\psi_{\rm g}(R,\tau_2)|^2$ in the spatial window $|F_{\rm sg}(R)\mu_{\rm sa}\mu_{\rm ag}|^2$ at the delay time τ_2. In this way, the quantum dynamics is reflected in the measured ion yields.

3 Results

3.1 Pump-dump population transfer

We first discuss the population transfer between the ground and excited electronic state, induced by the interaction with a pump- and a dump-pulse with frequencies corresponding to 638 nm (pump) and 685 nm (dump). Figure 2a shows the difference in the ground state population obtained in the case when both pulses interact ($P_{\rm g}(p/d)$) and in the case when only the pump pulse is present ($P_{\rm g}(p)$) as a function of delay time $\tau_1 = T_2 - T_1$. The curve shows that at certain delay-times the dump-pulse is able to transfer about 20% of the total population into the ground electronic state. A periodic variation with a period of 460 fs is obtained. This is obviously due to the vibrational motion of the excited state wave packet $\psi_{\rm e}$ as illustrated in Figure 2b. This figure displays the bond-length expectation value $\langle R\rangle_t$ in the state $|e\rangle$. A comparison with the population (Fig. 2a) shows that each time the $|e\rangle$-state wave packet is located around the outer turning

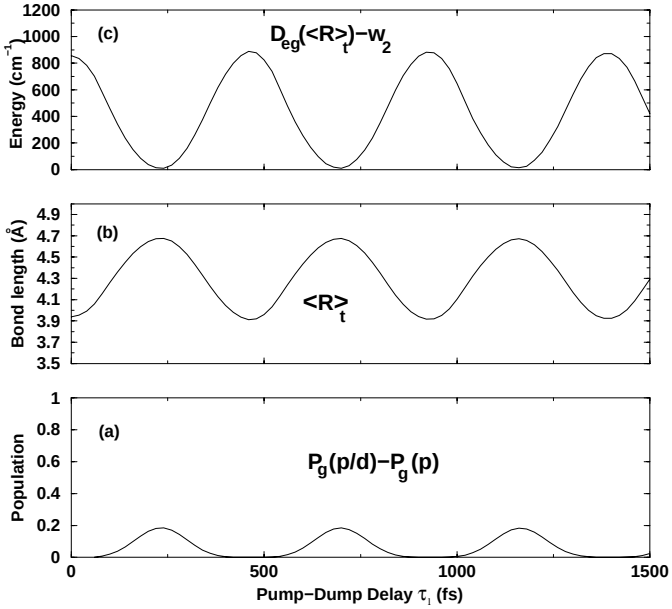

Fig. 2. Panel (a): difference in the ground state population created by the interaction with the pump- and dump-pulse ($P_{\rm g}(p/d)$) and the population obtained for the pump-pulse interaction ($P_{\rm g}(p)$). The curve is shown as a function of the delay time τ_1 between the pulses. Panel (b) contains the bond-length expectation-value in the electronically excited state $|e\rangle$, calculated at time τ_1. Panel (c): difference between the potentials in the states $|e\rangle$ and $|g\rangle$, reduced by the dump-pulse frequency and calculated at the expectation value as displayed in panel (b).

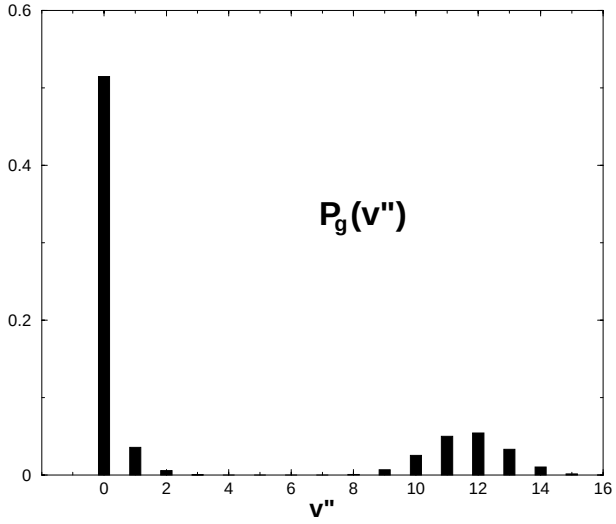

Fig. 3. Ground state vibrational distribution, obtained after the pump- and dump-pulse interaction for a delay time of $\tau_1 =$ 240 fs. The 638 nm pump pulse populates states with lower quantum numbers, whereas the dump pulse (685 nm) excites higher states in $|g\rangle$ at the time when the $|e\rangle$-state wave packet is located around the outer turning point of its vibrational motion.

point of its vibrational motion, the population transfer to the ground state is most effective. This was also concluded from the experimental results [9–11].

Using similar arguments as presented in Section 2, the ground state population created in the dump process can be approximately written as

$$P_{\rm g}(\tau_1) \sim \int {\rm d}R\, |F_{\rm eg}(R)\mu_{\rm eg}\psi_{\rm e}(\tau_1)|^2, \qquad (12)$$

with the Franck-Condon window defined as

$$F_{\rm eg}(R) = \frac{E_2}{2}\int {\rm d}t\; f(t){\rm e}^{-{\rm i}(V_{\rm e}(R)-V_{\rm g}(R)-\omega_2)t}. \qquad (13)$$

The FC-window $F_{\rm eg}(R)$ has its maximum at a distance where the difference potential $D_{\rm eg}(R) = V_{\rm e}(R) - V_{\rm g}(R)$ equals the laser carrier frequency ω_2. Thus the maximal population transfer is to be expected at times when the $|e\rangle$-state wave packet is located within the window. This is illustrated in Figure 2c which shows the function

$$D_{\rm eg}(\langle R\rangle_t) - \omega_2. \qquad (14)$$

As expected, the minima (being close to zero) of this function coincide with the maxima of the ground-state population.

It is interesting to analyze the ground-state distribution of vibrational states $|\varphi_{v''}\rangle$ after the pump-dump process. This distribution, defined as

$$P_{\rm g}(v'') = \frac{|\langle\varphi_{v''}|\psi_{\rm g}\rangle|^2}{\langle\psi_{\rm g}|\psi_{\rm g}\rangle}, \qquad (15)$$

is displayed in Figure 3 for a pump-dump delay of $\tau_1 =$ 240 fs. One clearly distinguishes a *cold* distribution consisting mainly of the vibrational levels with quantum numbers $v'' = 0$, 1 and a *hot* distribution with quantum numbers between 9 an 14. The latter contribution is prepared by the interaction with the dump-pulse which accesses higher energies within the ground-state potential. The particular structure of the vibrational distribution allows for a decomposition of the ground state wave packet into a cold ($|\psi_{\rm gc}\rangle$) and hot ($|\psi_{\rm gh}\rangle$) part as

$$|\psi_{\rm g}(t)\rangle = |\psi_{\rm gc}(t)\rangle + |\psi_{\rm gh}(t)\rangle\cdot \qquad (16)$$

The vibrational dynamics of $|\psi_{\rm g}(t)\rangle$ is now investigated by time-delayed ionization which is the subject of the next subsection.

3.2 Transient ion signals

We now turn to the calculated transient signals which were obtained within the approximations as discussed in Section 2. Figure 4 displays signals calculated using $|\psi_{\rm gc}(t)\rangle$ (panel (a)), $|\psi_{\rm gh}(t)\rangle$ (panel (b)) and the coherent sum $|\psi_{\rm g}(t)\rangle$ (panel (c)) as initial state for the probe process. The time-origin corresponds to the maximum of the pump-pulse envelope-function. The pump-dump delay was set to 240 fs and a 35 fs probe pulse with a carrier wavelength of 762 nm was employed in the calculation.

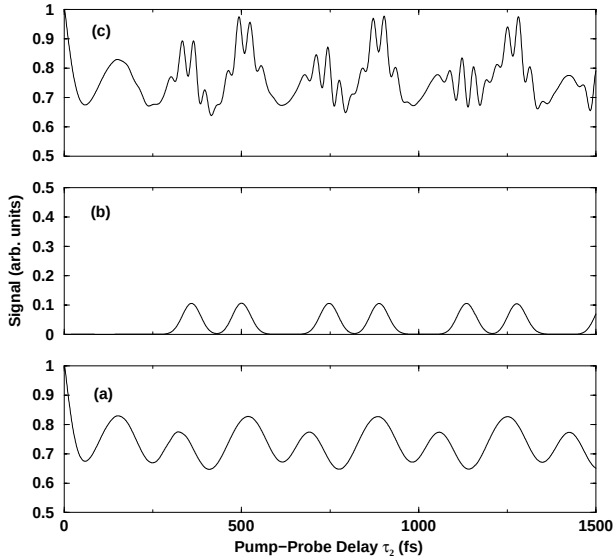

Fig. 4. Calculated pump-dump-probe signals as a function of delay time between the pump- and probe-pulse. The pump-dump delay τ_1 was set to 240 fs and wavelengths of 638 nm (pump), 685 nm (dump) and 762 nm (probe) were employed. The signals are obtained for ionization from the initial state $|\psi_{\rm gc}\rangle$ (cold contribution, panel (a)), $|\psi_{\rm gh}\rangle$ (hot contribution, panel (b)) and from the total ground state $|\psi_{\rm g}\rangle = |\psi_{\rm gc} + |\psi_{\rm gh}\rangle$ total signal, panel (c)).

The signal originating from the cold ground state wave-packet exhibits a small periodic variation on a large background (note that the vertical axis in Fig. 4a does not start at a value of 0). Since $|\psi_{\rm gc}(t)\rangle$ is a linear combination of very few eigenstates with low quantum numbers, it does not move much on the ground state potential. As a consequence, most of the probability amplitude remains in the Franck-Condon window, which is located close to the potential minimum of $V_{\rm g}(R)$, giving rise to a large background signal. Nevertheless, a dynamical behavior can be deduced from the figure, taking place with a period of 366 fs. The double-peak structure occurs since during one vibrational period the Franck-Condon region is filled twice.

The signal obtained from a probe-excitation with initial state $|\psi_{\rm gh}(t)\rangle$ (Fig. 4b) does not exhibit a background and oscillates with a period of 388 fs. Furthermore this signal is identical to zero for times before the dump pulse interacts with the sample.

From the temporal variation of the signal we may calculate vibrational wave numbers of 90 cm^{-1} and 85 cm^{-1}, corresponding to the motion of $|\psi_{\rm gh}(t)\rangle$ and $|\psi_{\rm gc}(t)\rangle$, respectively. This is consistent with the experimental findings taking the slightly different excitation wavelengths into account [10].

Since the total signal results from a coherent superposition of the amplitudes obtained from the two ionization pathways (using the wave packets $|\psi_{\rm gc}(t)\rangle$, $|\psi_{\rm gh}(t)\rangle$ as initial states), it exhibits interference patterns. The latter are easily understandable using an eigenfunction expansion of the wave packets as

$$|\psi_{{\rm g}n}(t)\rangle = \sum_n a_n {\rm e}^{-{\rm i}\epsilon_n t}|\varphi_n\rangle, \tag{17}$$

where $n = {\rm h}, {\rm c}$. Inserting equation (17) into the expression for the signal (Eq. (11)) one obtains

$$S(\tau_2) = \int {\rm d}R\, |F_{\rm sg}(R)\mu_{\rm sa}\mu_{\rm ag}|^2 \times \{|\psi_{\rm gh}(R,\tau_2)|^2 + |\psi_{\rm gc}(R,\tau_2)|^2 + S_{\rm hc}(R,\tau_2)\}, \tag{18}$$

where the interference term is of the form

$$S_{\rm hc}(R,\tau_2) = 2{\rm Re}\sum_{\rm h,c} {\rm e}^{{\rm i}(\epsilon_{\rm h}-\epsilon_{\rm c})\tau_2} a_{\rm h}^* a_{\rm c} \varphi_{\rm h}^*(R)\varphi_{\rm c}(R). \tag{19}$$

The corresponding oscillation period can thus be related to the energy difference between the vibrational energies of the two ground state wave packets. Taking the value corresponding to $\epsilon_{12} - \epsilon_0$ yields a time of 31 fs which matches the separation of the fast oscillations in the signal.

The above mentioned fast oscillations have not been seen in the experiment which, due to the temporal width of the probe pulse, is expected. If the motion of the wave-packets during the probe transition is included in the theoretical description or a longer probe pulse is employed, these features are washed out. Nevertheless here we encounter an interesting effect which shows that higher overtone motion in the ground electronic state can, in principle, be detected *via* the discussed pump-dump-probe scheme.

4 Summary

We have analyzed pump-dump-probe experiments on the potassium dimer. Employing time-dependent quantum calculations we were able to confirm conclusions inferred from experimentally detected transient ionization signals. The interaction of a first laser pulse prepares a wave packet in an electronically excited state of the molecule. Using a second, time-delayed pulse, it is possible to transfer population back into the electronic ground state. The efficiency of this dump-process depends, for a fixed dump-frequency, on the delay time between the two pulses. An appropriate choice of this time allows for the preparation of a superposition of states with high vibrational quantum numbers (hot contribution). The time-resolved ionization signals then reflect periodicities corresponding to the wave packet created in the dump process additionally to a (cold) wave packet consisting of a sum of vibrational states with small quantum numbers which is prepared in the pump process.

In calculating the signals we found that they exhibit interference structures. The latter stem from the two contributions to the ion signals which originate from ionization of the two ground-state wave packets (cold/hot). In this way one is able to see traces of vibrational overtone motion which, however, due to their high frequency are difficult to detect. To our knowledge this effect was never observed in neither a calculation nor an experiment.

This work was funded by the Deutsche Forschungsgemeinschaft within the SFB 347, TP C–2 and C–5. We gratefully acknowledge support by the Fonds der Chemischen Industrie.

References

1. W.S. Warren, H. Rabitz, M. Dahleh, Science **259**, 1581 (1993).
2. *Chemical Reactions and their Control on the Femtosecond Time Scale*, edited by P. Gaspard, I. Burghardt, Adv. Chem. Phys. **101** (Wiley, New York, 1997).
3. P. Brumer, M. Shapiro, Chem. Phys. Lett. **126**, 541 (1986).
4. P. Brumer, M. Shapiro, Ann. Rev. Phys. Chem. **43**, 257 (1992).
5. D.J. Tannor, S.A. Rice, J. Chem. Phys. **83**, 501 (1985).
6. D.J. Tannor, R. Kosloff, S.A. Rice, J. Chem. Phys. **85**, 5805 (1986).
7. A. Assion, T. Baumert, M. Bergt, T. Brixner, B. Kiefer, V. Seyfried, M. Strehle, G. Gerber, Science **282**, 919 (1998).
8. R.S. Judson, H. Rabitz, Phys. Rev. Lett. **68**, 1500 (1992).
9. H. Schwoerer, R. Pausch, M. Heid, W. Kiefer, Chem. Phys. Lett. **285**, 240 (1998).
10. R. Pausch, M. Heid, T. Chen, W. Kiefer, H. Schwoerer, J. Chem. Phys. **110**, 9560 (1999).
11. R. Pausch, M. Heid, T. Chen, H. Schwoerer, W. Kiefer, J. Raman Spectrosc. **31**, 7 (2000).
12. S. Rutz, S. Greschnik, E. Schreiber, L. Wöste, Chem. Phys. Lett. **257**, 365 (1996).
13. S. Rutz, R. de Vivie-Riedle, E. Schreiber, Phys. Rev. A **54**, 306 (1996).
14. H. Schwoerer, R. Pausch, M. Heid, V. Engel, W. Kiefer, J. Chem. Phys. **107**, 9749 (1997).
15. C. Nicole, M.A. Bouchene, C. Meier, S. Magnier, E. Schreiber, B. Girard, J. Chem. Phys. **111**, 7857 (1999).
16. T. Hornung, R. Meier, M. Motzkus, Chem. Phys. Lett. **326**, 445 (2000).
17. T. Baumert, V. Engel, C. Meier, G. Gerber, Chem. Phys. Lett. **200**, 488 (1992).
18. R. de Vivie-Riedle, K. Kobe, J. Manz, W. Meyer, B. Reischl, S. Rutz, E. Schreiber, L. Wöste, J. Phys. Chem. **100**, 778 (1996).
19. N.F. Scherer, A.J. Ruggiero, M. Du, G.R. Fleming, J. Chem. Phys. **93**, 2366 (1990).
20. N.F. Scherer, R.J. Carlson, A. Matro, M. Du, A.J. Ruggiero, V. Romero-Rochin, J.A. Cina, G.R. Fleming, S.A. Rice, J. Chem. Phys. **95**, 1487 (1991).
21. V. Blanchet, M.A. Bouchene, O. Cabrol, B. Girard, Chem. Phys. Lett. **233**, 491 (1995).
22. V. Blanchet, C. Nicole, M.A. Bouchene, B. Girard, Phys. Rev. Lett. **78**, 2716 (1997).
23. V. Blanchet, M.A. Bouchene, B. Girard, J. Chem. Phys. **108**, 4862 (1998).
24. M.D. Feit, J.A. Fleck, A. Steiger, J. Comp. Phys. **47** (1982) 412.
25. M. Lax, J. Chem. Phys. **20**, 1752 (1952).
26. M. Braun, C. Meier, V. Engel, J. Chem. Phys. **103**, 7907 (1995).
27. E.M. Hiller, J.A. Cina, J. Chem. Phys. **105**, 3419 (1996).
28. L.W. Ungar, J.A. Cina, Adv. Chem. Phys. **100**, 171 (1997).
29. S. Dilthey, S. Hahn, G. Stock, J. Chem. Phys. **112**, 4910 (2000).